Optics & Laser Technology 138 (2021) 106850

Contents lists available at ScienceDirect

Optics and Laser Technology

journal homepage: www.elsevier.com/locate/optlastec

Full length article

Synergistic effect in a two-phase laser procedure for production of silver nanoparticles colloids applicable in ophthalmology

A.S. Nikolov [a,*], N.E. Stankova [a], D.B. Karashanova [b], N.N. Nedyalkov [a], E.L. Pavlov [a], K. Tz. Koev [a,c], Hr. Najdenski [d], V. Kussovski [d], L.A. Avramov [a], C. Ristoscu [e], M. Badiceanu [e,f], I. N. Mihailescu [e]

[a] Institute of Electronics, Bulgarian Academy of Sciences, 72 Tsarigradsko Chaussee, Sofia 1784, Bulgaria
[b] Institute of Optical Materials and Technologies, Bulgarian Academy of Sciences, G. Bonchev Street, bl. 109, Sofia 1113, Bulgaria
[c] Department of Ophthalmology, Medical University - Sofia, 8 Bjalo more, Sofia 1000, Bulgaria
[d] The Stefan Angeloff Institute of Microbiology, Bulgarian Academy of Sciences, 26 Georgi Bonchev str, 1113 Sofia, Bulgaria
[e] National Institute for Lasers, Plasma and Radiation Physics, PO Box MG-36, RO-77125, Magurele, Ilfov, Romania
[f] University of Bucharest, Faculty of Physics, RO-77125, Magurele, Ilfov, Romania

ARTICLE INFO

Keywords:
Ultrafine silver nanoparticles
Laser ablation in water
Aqueous silver nanocolloids
Post-ablation irradiation
Antibacterial action
Ophthalmological application

ABSTRACT

This paper reports on the production of Ag nanoparticles (AgNPs) in a water solution based on a two-phase pulsed laser procedure in view of therapeutic ophthalmological applications requiring AgNPs size of ≤10 nm with a narrow size distribution. Nanoparticles of this size scale are capable of penetrating the complex ocular barriers, thus ensuring effective non-invasive drug delivery to the retina. Moreover, the ocular irritation, which is currently associated to the conventional ocular drug administration routes, would be avoided.

In the first phase, AgNPs larger than 20 nm were fabricated via laser ablation of a Ag target in water by irradiation with the fundamental wavelength (λ = 1064 nm) generated by a Nd:YAG laser. During the second phase, to reduce the mean size of the as-obtained nanoparticles and properly adjust the size distribution, the water colloids were additionally irradiated with the ultraviolet harmonics (355 nm and 266 nm) of the same laser source. The effect of the key laser parameters - wavelength, fluence and laser exposure time - upon the nanoparticles morphology was studied. The most suitable post-ablation treatment of initial colloids was obtained by a consecutive irradiation with the third (λ = 355 nm) and the fourth (λ = 266 nm) harmonics of the fundamental laser wavelength. By using this approach, a synergistic effect between two mechanisms of light absorption by AgNPs was induced. As a result, contaminant-free colloids of AgNPs with sizes of less than 10 nm and quite a narrow size distribution with a standard deviation of 1.6 nm were fabricated.

The toxic effect of the as-produced AgNPs on Gram-positive and Gram-negative bacteria and *Candida albicans* was explored. The most efficient action was reached against *Pseudomonas aeruginosa* and *Escherichia coli*.

A potential application was proposed of the synthesized AgNPs colloidal aqueous solutions with antimicrobial action as a non-invasive method for ocular infections prevention and treatment.

1. Introduction

The unique electronic [1,2], optical [3,4], magnetic [5–7] and catalytic properties [8,9] of noble metals nanoparticles, essentially different from those of the bulk material, have attracted considerable research interest. It encompasses various fields, from fundamental sciences, such as physics (surface plasmon resonance (SPR) in visible and near UV regions or plasma discharge enhancement) [10], chemistry (catalysis) and biology (optical markers for diagnosis of various biological objects), to applied sciences, as design and development of a variety of electronic devices and sensors, and to industrial areas, as textile and cosmetics industry.

In what concerns silver particles of nanometer size (AgNPs), besides being nontoxic, they are known to suppress or destroy various types of bacteria [11]. Thus, they have provoked particular and wide-ranging interest for medicinal uses, e.g., improving the anti-bacterial effect of

* Corresponding author.
E-mail address: anastas_nikolov@abv.bg (A.S. Nikolov).

https://doi.org/10.1016/j.optlastec.2020.106850
Received 30 June 2020; Received in revised form 31 October 2020; Accepted 12 December 2020
Available online 21 January 2021
0030-3992/

antibiotics [12], or as components in unguents for skin application [13]. Their size is smaller than that of human cells by several orders of magnitude, which is opening unique opportunities for biochemical interactions, either on the cells' surface or within cells [14]. Elechiguerra et al. [15] described AgNPs interacting with the HIV-1 virus thus suppressing in vitro its attachment to cells. Furthermore, silver nano-sized particles were found to inhibit the process of forming advanced glycation end-products, which could alleviate the adverse effects of diabetes [16]. Recently, these particles' beneficial capability in treating malignancies, and in diagnostic and probing were recognized [17]. This list of applications of silver nanoparticles, emphasizing their use in medicine, is relevant to the thematic orientation of the article. Their application in other areas is much wider, e.g.: a) detection by surface enhanced Raman spectroscopy (SERS) of ultra-low concentration of some molecules attached to AgNPs [18,19]; b) microelectronics; c) sunscreens and cosmetics [20,21]; d) clothing [22,23], etc. The increased interest in AgNPs due to their extremely wide range of applications led to development of various methods for their fabrication. In general, they can be classified as chemical [24], photochemical [25], electrochemical [26], sonochemical [27], biological [28], or physical [29]. The potential toxicity of the residual ions as byproducts in colloids produced by various chemical methods remains a common disadvantage with respect to further biological application. The inability to fabricate large quantities of AgNPs is the major limitation of biological synthesis. Vacuum conditions and very high temperature associated with expensive equipment are connected as a rule with the use of physical methods. In this context, one promising physical method for fabrication of AgNPs colloids for medical applications is pulsed laser ablation in liquids (PLAL) [30]. A major advantage of this method is the fabrication of contamination-free colloids by using a simple and low-cost processing setup. The main disadvantage of PLAL approach compared to the other fabrication methods is the wider size distribution of the nanoparticles produced.

The object of this study is fabrication of Ag nanocolloids for drug delivery in ophthalmology. As known, the passage of drugs in the form of eye drops to the posterior segment of the eye is severely restricted by eye barriers. Several ways of delivering drugs to the eye are currently being used: topical infusion and sub-conjunctival injection, trans-scleral drug delivery, intra-vitreal injection, sub-retinal injection [31,32]. The above-mentioned invasive methods may sometimes lead to post-administration complications, such as intraocular infections and retinal detachment. Nanoparticle delivery systems can reduce the incidence of injections and intraocular complications. In this case, the nanoparticles size is a key factor for ocular drug delivery efficiency. Bisht et al. [33] showed that the size of scleral water channels/pores is about 30–300 nm. Particles smaller than 20 nm can penetrate the corneal endothelium, which is the first eye barrier [34]. A narrow size distribution of NPs with sizes of less than 10 nm is an important requirement for NPs to serve as successful blood-retinal barrier transporters in eye drug delivery. This condition can be implemented via irradiating already-fabricated colloids with laser light under optimized parameters (wavelength, time of laser exposure and fluence, the later defined as the ratio between the laser pulse energy and the laser spot area) [35,36]. Such an approach (the so-called pulsed laser irradiation in liquids (PLIL) method) has been employed mostly in laser synthesis of gold NPs to modify both their size-distribution and morphology [37–40]. The irradiation procedure could be conducted by either nano-, pico- or femtosecond lasers [41–44], taking into account the corresponding type of laser-mater interaction in nanoscale range.

We report on a simple approach for fragmentation of silver NPs by post-laser ablation treatment of water Ag nanocolloids via consecutive laser irradiation with 355 nm and 266 nm nanosecond pulses generated by the Nd:YAG laser source. Using this approach, for the first time to the best of our knowledge, contaminant-free AgNPs were fabricated with a size below 10 nm and a very narrow size distribution, namely, with a mean diameter of 5.4 nm and a standard deviation of 1.6 nm. The AgNPs produced completely conform to the ophthalmology demands for blood-retinal barrier transporters in eye drug delivery. Our investigation by a microbiological assay established strong antibacterial and antifungal activity of the newly fabricated Ag nanoparticle colloids. The potential application of the synthesized AgNPs colloidal aqueous solutions with antimicrobial action was proposed as a non-invasive method for ocular infections prevention and treatment.

2. Materials and method

Our studies were organized in two steps: i) synthesis of AgNPs in a water solution by multiple laser ablation of a silver target in water (PLAL method) with the fundamental wavelength of a multimode Nd:YAG source to produce the initial colloids; ii) controlled modifications of AgNPs by a subsequent irradiation with the 355-nm and 266-nm harmonics (PLIL method) of the same laser source.

Indeed, according to Drude's theory [45], the coupling of laser light with metals strongly depends on the wavelength. In particular, Ag strongly reflects IR (1064 nm) radiation and intensively absorbs in the UV (355 nm and 266 nm) range. This is why in our experiments the 1064 nm radiation was focused (in a spot of ~0.0095 cm^2), while the 355-nm and 266-nm radiations were unfocused.

The idea was to use the first phase (1064 nm) to excavate and evacuate large NPs from the crater forming on the Ag target surface, while the other two beams (355 nm and 266 nm) of 6-mm diameter (a spot of ~0.2826 cm^2) intercept quite a large number of the generated NPs and breaks them into smaller fragments.

In our opinion, the UV radiation can be more efficient in breaking rather large AgNPs. This behavior can attenuate, if not cancel, the opposite effects due to the close vicinity of the 266 nm wavelength to the inter-band transition and that of 355 nm not corresponding to a high absorption of the SPR.

The experiments were conducted as follows:

2.1. *Ag nanoparticle colloids: fabrication in water – "first phase"*

A pure silver target (99.99% purity, with a diameter of 30 mm and a thickness of 2 mm) was subjected to multiple Nd:YAG laser irradiation at $\lambda = 1064$ nm with 15-ns laser pulses at a frequency repetition rate of 10 Hz. Prior to immersion, the target was cleaned for 10 min in an ultrasonic bath: several times with distilled water, once with ethanol and again with water.

The target was placed on the slightly conical bottom of a polypropylene vessel and immersed in 10 mL double-distilled water (0.8 μS m^{-1}) at 6 mm below surface. To position the target horizontally, an appropriate round Teflon® holder was manufactured. The upper side of the holder was softly carved to accommodate the target. The target was not fixed on the bottom, but was left free under its own weight. However, its horizontal movement was limited by the walls of the nest. 1800 consecutive laser pulses were applied for synthesis of AgNPs in the solution. In order to keep the ablation efficiency at a reasonable level, the fluence was gradually increased during the multiple irradiation, from the initial value of 20 J/cm^2 to the final value of 26.8 J/cm^2 for a total irradiation time of 3 min. The intermediate values and corresponding irradiation times were found experimentally after optimization and are summarized in Table 1. The laser beam was focused by a lens ($f = 22$ cm) normally to the disc-shaped silver target. A separation distance of 18 cm was chosen. The experimental setup employed to fabricate the initial AgNPs colloids is presented schematically in Fig. 1 and is similar to the one described in Nikov et al. [46]. In the present experiment, the target was mounted on a computer-controlled stepper-motor *x-y* table. The precise control of the target translation motion provided an operating mode which corresponds to 10 overlapping pulses per laser beam spot. In the first phase, the laser beam was focused and the diameter of the spot on the target surface was ~0.0095 cm^2. The laser energy per pulse varied from 190 mJ to 255 mJ, corresponding to a laser fluence in the range 20.0–26.8 J/cm^2.

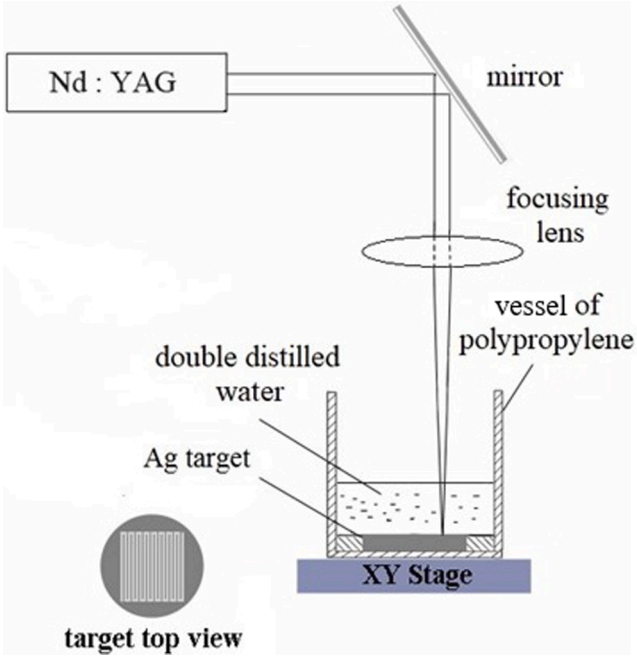

Fig. 1. Experimental set-up used in the first phase (1064 nm) of the multi-pulse laser generation of AgNP colloids.

2.2. Fragmentation of initial colloids by third and fourth harmonics of Nd:YAG laser source – "second phase"

In the second phase of the experimental procedure, in order to fragment the silver nanoparticles the initial colloids were irradiated with the third ($\lambda = 355$ nm) and the fourth ($\lambda = 266$ nm) harmonics generated by the same Nd:YAG laser source.

In this case, the laser beam was not focused and the diameter of the spot was ~6 mm (laser spot area of 0.2826 cm^2). The laser pulse energy was varied from 18.5 mJ to 68 mJ at 355 nm and 4.6 mJ to 9.4 mJ at 266 nm. The corresponding laser fluence was in the range (0.05–0.07 J/cm^2) for 355 nm and of 0.02 J/cm^2 for 266 nm, i.e. about three orders of magnitude lower than in first phase.

It requires a certain time (number of pulses) to irradiate all nanoparticles in the liquid. For a given laser fluence, the colloids pass through various intermediate states until an equilibrium is reached, which can be detected by the changes in the profile of the optical transmission spectrum. The transition can be monitored and controlled via the irradiation time (Table 1). These two wavelengths were selected since they are located close to the plasmon and to the interband absorption [47] peaks of AgNPs, respectively. The experimental set-up was similar to the one described in Nikolov et al. [35]. The colloids were stored in a container rotating at a frequency of 4.3 rpm. The unfocused laser beam was directed normally to the top surface of colloids. The experiments of the second phase were conducted by irradiating the initial colloid under three different modes. In the *first two modes*, the colloid was irradiated with either the wavelength of 355 nm or with the wavelength of 266 nm only. According to our studies, both modes reduce the AgNPs mean size and narrow their size distribution in a different way, but not appropriate for the medical application discussed above.

Combined irradiation was therefore applied in the *third mode*, by using sequentially the wavelengths of 355 nm and 266 nm. To the best of our knowledge, this procedure was for the first time applied to reach the main goal of the treatment – fabricating a colloid suitable for use in ophthalmology (Patent application) [48]. The laser fluence and irradiation times were found experimentally after optimization. These data are collected in Table 1. The total irradiation time was determined based upon the effect of laser treatment on AgNPs optical transmission spectra obtained during the previous step. The optical transmission of colloids was measured after each step of irradiation lasting 5 min according to the procedure described in Nikolov et al. [35]. It showed the evolution of the transmission spectra as the time of laser exposure was increased.

Table 1
Numerical values of important technological parameters of the laser beam used in the different experimental phases.

Experimental phase	Mode	Laser wavelength [nm]	Laser beam spot area [cm^2]	Laser fluence [J/cm^2]	Time of exposure [min]
I focused laser beam		1064	0.0095	20.0	0.83
				21.0	0.67
				23.7	0.67
				24.7	0.67
				26.8	0.16
II unfocused laser beam	1	355	0.2826	0.059	85
				0.068	5
	2	266		0.023	55
	3	355		0.059	85
				0.068	5
		266		0.02	20

2.3. Physical-chemical characterization of Ag nanoparticles

The optical transmission spectra of AgNPs water colloids in the UV/Vis range (200–900 nm) were recorded by an Ocean Optics HR 4000 spectrometer. The size and the morphology of AgNPs were visualized by transmission electron microscopy (TEM). The images were acquired by a JEOL JEM 2100 at an accelerating voltage of 200 kV. High-resolution transmission electron microscopy (HRTEM) and selected area electron diffraction (SAED) were used to characterize the nanoparticles microstructure and their phase composition.

2.4. Ag nanoparticles: Microbiological assay

The antibacterial and antifungal activity of the newly fabricated Ag nanoparticle colloids were assessed by using Gram-positive and Gram-negative bacteria and Candida albicans. The following strains were used: *Staphylococcus aureus* strain 29213 and *Escherichia coli* strain 35218 from an American Collection of Cell Cultures (ATCC); *Pseudomonas aeruginosa* strain 1390 and *Candida albicans* strain 74 from the collection of the Stefan Angeloff Institute of Microbiology, Bulgarian Academy of Sciences. Suspensions of the respective microorganisms with a concentration of 1×10^6 CFU mL^{-1} were prepared. The experiments were conducted with an incubation mixture containing equal volumes of suspensions of microorganisms and AgNPs. The mixture was poured in 12-well polystyrene plates, continuously shaken, and sampled at pre-defined intervals (0, 2, 5 and 24 h) in order to count the number of viable microorganisms. Tenfold diluted solutions of the incubation mixtures in a nutrient medium (Tryptic soy agar, Oxoid) were seeded and the colonies-forming units (CFUs) were counted after culturing for 24 h at 37 °C.

To confirm the results, the experiments were repeated three times, with numerical values presented as an average value +/- mean standard deviation (SD). The difference between the two means was determined by a two-tailed unpaired Student's test.

3. Results and discussion

3.1. Photo fabrication of Ag nanocolloids

Fig. 2 shows the typical TEM micrographs (a), distribution histograms (b) and the corresponding SAED patterns (c) of the AgNPs obtained after pulsed laser ablation and following irradiation, respectively, in water environment. They were organized in the respective order: Ag

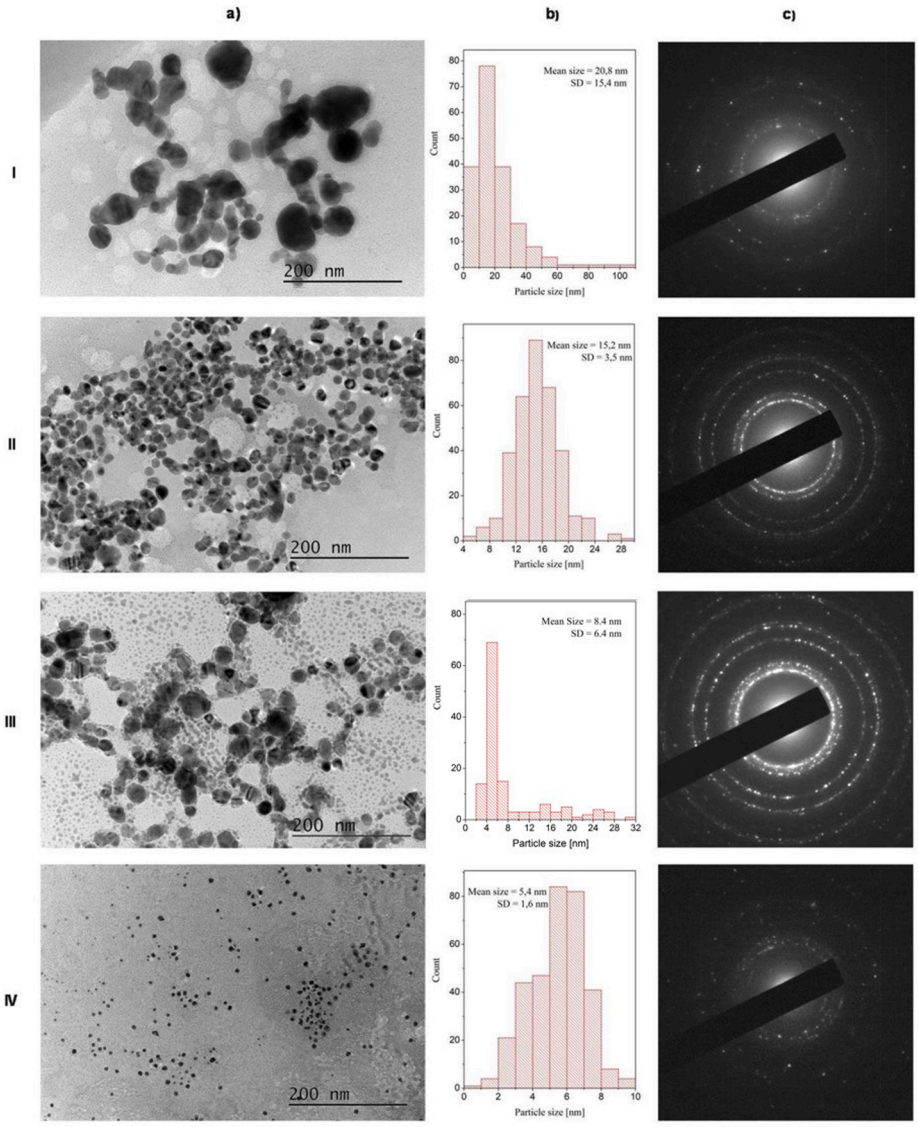

Fig.2. a) Typical TEM micrographs, b) particles' size distribution histograms, c) corresponding SAED patterns of Ag colloids produced after the first phase (I) – initial colloid, and the second phase (II) with 355 nm – after 85 min, 266 nm (III) – after 40 min, and consecutive application of 355 (after 85 min) and 266 nm (after 15 min) wavelengths laser pulses, respectively – (IV).

colloids after the *first phase* (I) and after *second phase* (II-IV), which corresponded to the three modes of UV irradiation introduced above.

Fig. 2 I-a is indicative for spherical and spherical-like AgNPs shapes of the initial colloid prepared during the ablation process in the first experimental phase. Also, formation of aggregates was observed. Ag grains with a mean size of ~20 nm (Fig. 2 I-b) exceeds by a factor of more than two the upper limit of the proper size needed for the specific medical application [33–34].

As expected, the application of the second phase resulted in fragmentation of AgNPs. This demonstrates a significant predominance of initial NPs splitting against their growth by coalescing for the selected values of multiple laser irradiation parameters in the second phase. As a result, a mean NPs size of 15.2 nm, 8.4 nm after irradiation with 355 nm, 266 nm only and 5.4 nm after the consecutive irradiation with wavelengths of 355 nm and 266 nm for the three irradiation modes were obtained, Fig. 2II-IV. The SD decreased significantly in all cases after the second phase (3.5, 6.4 and 1.6 nm) with respect to the first phase (15.4 nm). It is noteworthy that the smallest mean size and SD values were observed after the consecutive irradiation with wavelengths of 355 nm and 266 nm (the third irradiation mode), Fig. 2-IV.

The total number of nanoparticles used to compile the histogram can be derived directly from Fig. 2: I-b) - about 200, II-b) – about 340, III-b) – about 125, IV-b) – about 690.

The SAED patterns indicate a polycrystalline structure because of the small particle size. While the SAED patterns' indexing confirmed the presence of a unique phase – cubic silver, with lattice parameter a = 4.0855, conforming to Entry # 96-110-0137 of free-of-charge crystallography open database (COD), incorporated in Match software, Fig. 2c.

As visible in Fig. 2, the number of elongated nanoparticles are prevalent after the first phase. When continuing with the second phase, they are gradually converted to become completely spherical after the subsequent irradiation with the two short wavelengths (355 nm and 266 nm). Figs. 3–5 displays the optical transmission of the colloidal solutions produced under different irradiation conditions.

In Fig. 3 one can see the changes in the transmission of the colloidal solutions after the first phase (a) and the second phase with $\lambda = 355$ nm and a fluence of 0.059 J cm^{-2} for 30 (b), 50 (c), 70 (d) and 85 (e) minutes of irradiation time. For comparison, the fluence was raised up to 0.068 J cm^{-2} and the colloid was exposed to further five minutes (total irradiation time of 90 min) (Fig. 3f). The following can be concluded by

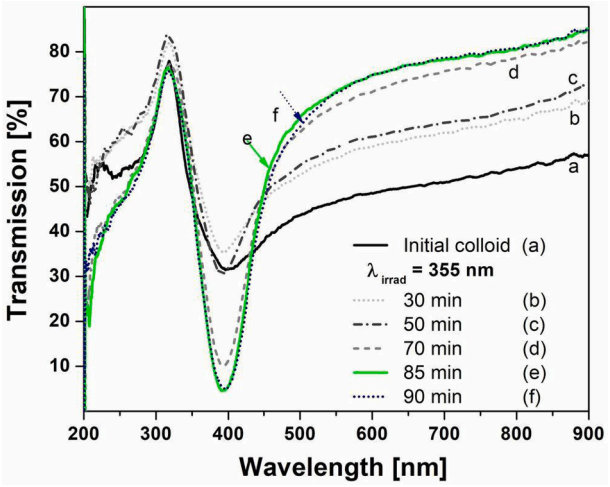

Fig. 3. Optical transmission spectra of AgNPs aqueous colloids: a) initial colloid after laser ablation with 1064 nm followed by irradiation with 355 nm after: b) 30 min, c) 50 min, d) 70 min, e) 85 min, f) 90 min.

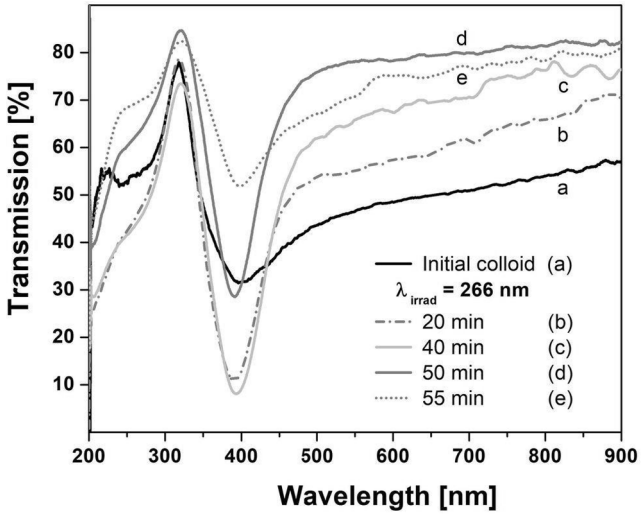

Fig. 4. Optical transmission spectra of AgNPs aqueous colloids: a) initial colloid after laser ablation with 1064 nm and after the subsequent laser irradiation with 266 nm for: b) 20 min, c) 40 min, d) 50 min, e) 55 min.

analyzing the data in Fig. 3:

The transmission was the lowest in the case of the initial colloid produced in the first phase.

It gradually increased with the number of subsequent laser pulses (total time duration) applied during the second phase.

Saturation appeared when duration exceeded 85 min, even when the laser fluence was increased to 0.068 J cm^{-2} (Fig. 3f).

A prominent band within the range of 300–600 nm with a minimum at ~390 nm is present in all spectra. This band should be most probably assigned to surface plasmon resonance (SPR) associated with absorption by free electrons in the silver nanoparticles [49]. It confirms the correlation between the SPR characteristics and the mean size and distribution of NPs [50]. After completion of each irradiation step, the SPR band progressively narrowed, the value of its minimum decreased and a spectrum shoulder extension towards the high-wavelengths region arose. This behavior was caused by a size-redistribution in the ensemble of nanoparticles, which might be due to the relatively low laser fluence values used in our experiments, in accordance with the "particle heating-melting-evaporation" model proposed by Takami et al. [51]. As is well-known, the NPs absorption depends on their geometric cross-

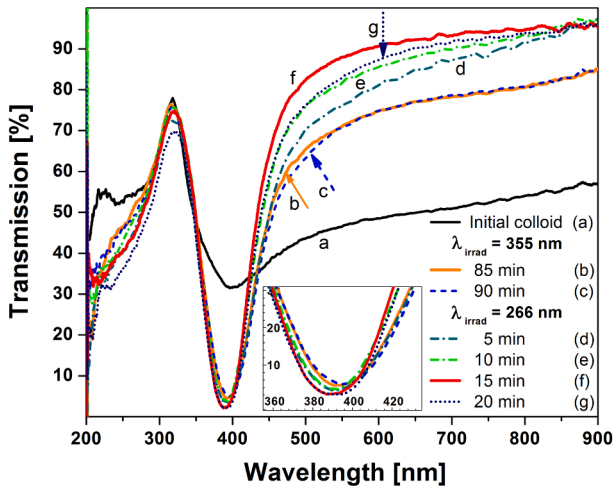

Fig. 5. Optical transmission spectra of AgNPs aqueous colloids: a) initial colloid after laser ablation with 1064 nm and consecutive laser irradiation with 355 nm after: b) 85 min, c) 90 min, followed by 266 nm for: d) 5 min, e) 10 min, f) 15 min, g) 20 min.

section, i.e. size conditioned by dumping and retardation effects and the SPR position with respect to the incident radiation wavelength. Moreover, the smaller NPs in water colloids are characterized by a higher heat-dissipation rate to the surrounding water [43,50,52] because of the increased surface/volume ratio.

The laser treatment of colloids initiates two concurrent processes: fragmentation of big nanoparticles and the concomitant aggregation and fusion of small ones. The energy of the electrons excited by SPR is transferred to the lattice by electron-phonon coupling. When the temperature reaches the melting point, latent heat should be further delivered to reach a complete melting of the NPs. The temperature rise continues to the boiling and evaporation point, which also needs latent heat compensation and results in a reduction of the AgNPs mean size by selective fragmentation of the biggest ones. On the other hand, fusion of NPs can proceed by aggregation and melting.

The equilibrium between these two processes, fragmentation and fusion, depends on the laser pulse energy and on the duration of irradiation and affects the NPs mean size and size distribution. In the case discussed, the reduction trend of these characteristics of the NPs ensemble continued up to 85-min irradiation duration, as evidenced by the optical transmission spectra in Fig. 3e. During the pulsed laser exposure, the fragmentation tendency obviously dominated the particle-size redistribution evolution. However, the following increase of the irradiation time and/or laser fluence led to a widening of the plasmon band in the transmission spectrum. This could be the result of enhanced aggregation and fusion of AgNPs.

The application of the second mode of illumination was therefore extended in order to preserve the photo-fragmentation predominance. It was conducted in a way analogous to the previous one ($\lambda = 355$ nm), except for the use of the more energetic photons of the fourth harmonic ($\lambda = 266$ nm or 4.66 eV, as compared with 3.49 eV for 355 nm). Very importantly, the SPR absorption was replaced in this case by an absorption process due to an inter-band transition [47].

Fig. 4 displays the results obtained by optical transmission spectroscopy after the two steps of laser irradiation, i.e. initial colloids generation by 1064 nm followed by AgNPs fragmentation under 266-nm irradiation for different irradiation times. One can see a tendency similar to that observed in Fig. 3, i.e., a progressive narrowing of the SPR band and a rise of the spectrum wing in the long-wavelengths region. Nevertheless, saturation appeared again after about 50 min of irradiation. It is followed by a reverse trend of increasing NPs size and widening of the size distribution.

The best AgNPs colloids were obtained after 40 min of irradiation

(Fig. 4, spectrum "c") but the particles' mean size was still unsuitable for ophthalmologic applications.

Another feature that should be mentioned when comparing the TEM images obtained in the two measurement modes was the appearance of two populations of nanoparticles – bigger and smaller. This process was barely noticeable in the first irradiation mode (Fig. 2-II), but was very pronounced in the second one (Fig. 2-III), which was reflected in the relatively wide nanoparticles' size distribution in this case. The standard deviation value (6.4 nm) of the AgNPs mean size in the colloid obtained after irradiation with only 266 nm (second mode) is nearly twice the standard deviation (3.5 nm) of the average size of nanoparticles obtained after irradiation with only 355 nm (first mode).

One should conclude that the first two modes of laser irradiation reduced the AgNPs mean size and narrowed their size distribution in different ways, without being able however to fully meet the specific requirements for medical use in ophthalmologic therapy.

This is why we used a combined treatment by the third ($\lambda = 355$ nm) and the fourth ($\lambda = 266$ nm) harmonics successively applied for irradiation of the initial colloid in the third mode of the second phase of the experimental procedure. It was organized in analogy with the first two modes. The initial colloid was irradiated during the first 85 min with $\lambda =$ 355 nm at the same laser energy as in Fig. 3. The change of the optical transmission spectrum of the initial colloid after 85 and 90 min of irradiation with 355 nm is seen in Fig. 5.

The irradiation was continued with 266 nm for different durations. A certain narrowing of the plasmonic band was observed after 5 min and 10 min irradiation time. Reducing the number of large particles should lead to an increase in the transmission values in the long wavelengths region of the spectrum, which was in fact observed. The maximum effect was reached after 15 min laser irradiation (Fig. 5, spectrum "f").

Prolonging further the irradiation duration caused the reverse trend, as evidenced by the optical transmission spectrum after 20 min (Fig. 5g). The average size of the silver nanoparticles produced in the third mode and its corresponding standard deviation (5.4 nm and 1.6 nm, respectively) were the smallest ones compared with those of the AgNPs produced in the first and second modes. This proved that a synergistic effect was reached with the third mode of irradiation combining the consecutive actions of the two mechanisms of absorption mentioned above in what concerns the AgNPs average size and size distribution.

Very importantly, the TEM examination showed that the nanoparticles generated preserved the spherical shape in this case, too (Fig. 2a).

In conclusion, the *third mode* completely meets the goal of the treatment, i.e., preparation of silver nanocolloids suitable for use in ophthalmology. Thus, the fabrication of nearly monodisperse Ag nanoparticles with an average size of 5.4 nm would allow the drugs in the form of eye drops to pass through most of eye barriers, such as scleral water channels/pores, and penetrate the corneal endothelium [33–34].

The stability of all colloids generated was studied in Nikov et al. [53], where results are presented for 30 days of observation. The changes in the colloids consisted in aggregation of the nanoparticles and their subsequent settling on the bottom of the storage vessel.

3.2. Antimicrobial assay

The results reported in this Section were obtained with AgNPs of ~5.4-nm mean size produced using the third irradiation mode under optimum conditions.

The studies showed that the AgNPs were the most effective against *Pseudomonas aeruginosa*. They reduced the number of bacteria by four logs (10,000 times, i.e., lower than the minimum level of viable microorganisms, (Fig. 6) after two hours. Then, the number of viable bacteria dropped fast and after five hours they were completely inactivated. A very effective action was obtained against *Escherichia coli* for which full inactivation was also observed after five hours. The process of inactivation ran rapidly between the second and the fifth hour (Fig. 7).

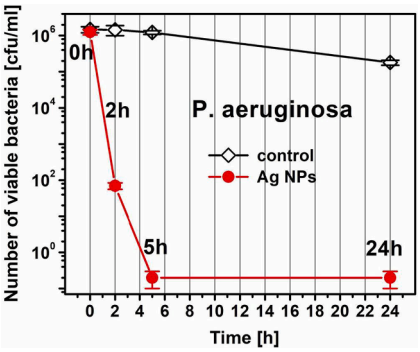

Fig. 6. Antibacterial action of AgNPs produced by the third mode of irradiation against *Pseudomonas aeruginosa*. The number of viable bacteria decreased 10,000 times after the 2-nd hour, while full inactivation was reached after the 5-th hour.

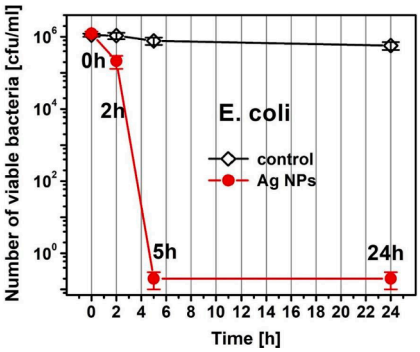

Fig. 7. Antibacterial action of AgNPs produced by the third mode of irradiation against *Escherichia coli*. Full inactivation was obtained after the 5-th hour.

The Ag nano-colloids reduced the number of *Staphylococcus aureus* approximately 10 times after five hours and completely inactivated the bacteria after 24 h (Fig. 8).

The antifungal action against *Candida albicans* started actively after five hours. The number of fungi was reduced approximately 150 times. The process continued for 24 h, when the fungi were completely inactivated (Fig. 9).

The antibacterial action of silver has been widely documented [54–56], although the exact mechanism causing it is still not completely understood. It is believed that it might derive from the inactivation of enzymes essential for the respiratory chain of the pathogen, or by generating hydroxyl radicals [57]. The latter cause, in turn, pathogens annihilation.

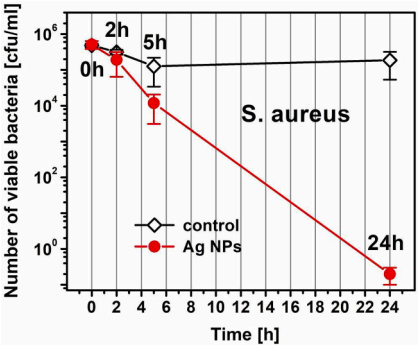

Fig. 8. Antibacterial action of AgNPs produced by the third mode of irradiation against *Staphylococcus aureus*. The inactivation process started after 5 h. The number of viable bacteria decreased about 10 times (viable microbes are below the minimum). Full inactivation was reached after 24 h.

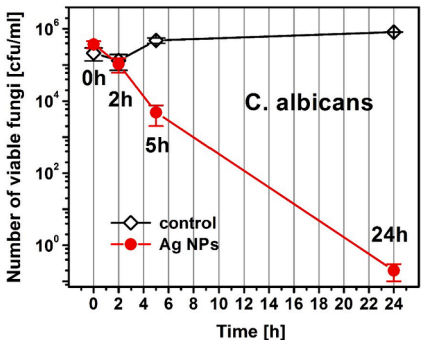

Fig. 9. Antifungal action of AgNPs produced by the third mode of irradiation against *Candida albicans*. Full inactivation was obtained after 24 h. The number of viable fungi decreased about 150 times after 5 h.

4. Conclusions

Pulsed laser ablation under different irradiation regimes was applied to produce Ag nano-colloids with controlled mean size and distribution suitable for potential ophthalmological applications.

To the best of our knowledge, a consecutive application of the third and the fourth harmonics after the fundamental wavelength of a Nd:YAG laser source was for the first time investigated with this purpose. It proved efficient in initiating synergistic effects arising from the consecutive application of the fundamental and the harmonics (third and fourth ones) to the same Ag nano-colloidal population. Under the optimal experimental conditions – consecutive laser irradiation of the water colloids of silver nanoparticles with 355 nm and 266 nm – chemicals-free AgNPs were formed with a mean size of 5.4 nm and a very narrow size distribution (standard deviation of ~1.6 nm).

The antibacterial action of AgNPs was explored showing good results against *Pseudomonas aeruginosa*, *Escherichia coli*, *Staphylococcus aureus* and *Candida albicans*.

The Ag nano-colloids proved most efficient against the *Pseudomonas aeruginosa* and *Escherichia coli* bacteria, for which full apoptosis was reached after five hours.

The small size of the AgNPs allows one to expect that their use would result in an efficient treatment of intraocular infections.

One should emphasize the key role of the laser pulse energy in narrowing the AgNPs size distribution after a multiple laser irradiation.

Our results provide a proof of the possibility to carry out an efficient environmentally-friendly multistep laser procedure of fabrication of ultrafine monodisperse Ag nanoclusters that can be used in non-invasive methods of prevention and treatment of several types of intraocular infections.

One should also note that the laser light used in all phases of the process – i.e. for both initial generation of Ag nano-colloids and the following adjustment of their size and size distribution (1064 vs. 355 and 266 nm) – were emitted by the same Nd:YAG laser source. This fact might have implications in devising low-cost technologies for the large-scale production of Ag nano-colloids.

Declaration of Competing Interest

The authors declare that they have no known competing financial interests or personal relationships that could have appeared to influence the work reported in this paper.

Acknowledgements

The research equipment used is part of the INFRAMAT distributed research infrastructure (part of the Bulgarian national roadmap for research infrastructures) supported by the Bulgarian Ministry of Education and Science under contract D01-382/18.12.2020. This work was partially supported by the Bulgarian National Science Fund at the Ministry of Education and Science (Contract No. KP- 06-H 38/13, 06.12.2019, "Development of biophotonics methods as the basis of oncology theranostics - 2").

The Romanian co-authors acknowledge the financial support by the Romanian Ministry of Education and Research under Romanian National Nucleu Program LAPLAS VI – contract no. 16N/2019. The bilateral cooperation between the Romanian and Bulgarian Academies of Sciences is also acknowledged under project "Laser-assisted processing of materials and their characterization for high technology applications" (2020-2022).

References

[1] D. Chen, X. Qiao, X. Qiu, J. Chen, Synthesis and electrical properties of uniform silver nanoparticles for electronic applications, J. Mater. Sci. 44 (2009) 1076–1081.

[2] A.H. Alshehri, M. Jakubowska, A. Młożniak, M. Horaczek, D. Rudka, C. Free, J. D. Carey, Enhanced electrical conductivity of silver nanoparticles for high frequency electronic applications, ACS Appl. Mater. Interfaces 4 (12) (2012) 7007–7010, https://doi.org/10.1021/am3022569.

[3] S. Eustis, M.A. El-Sayed, Why gold nanoparticles are more precious than pretty gold: Noble metal surface plasmon resonance and its enhancement of the radiative and nonradiative properties of nanocrystals of different shapes, Chem. Soc. Rev. 35 (2006) 209–217, https://doi.org/10.1039/B514191E.

[4] C. Noguez, Surface plasmons on metal nanoparticles: the influence of shape and physical environment, J. Phys. Chem. C 111 (2007) 3806–3819, https://doi.org/10.1021/jp066539m.

[5] J.S. Garitaonandia, M. Insausti, E. Goikolea, M. Suzuki, J.D. Cashion, N. Kawamura, H. Ohsawa, I. Gil de Muro, K. Suzuki, F. Plazaola, Chemically induced permanent magnetism in Au, Ag, and Cu nanoparticles: localization of the magnetism by element selective techniques, Nano Lett. 8 (2008) 661–667, https://doi.org/10.1021/nl073129g.

[6] H. Le Trong, K. Kiryukhina, M. Gougeon, V. Baco-Carles, F. Courtade, S. Dareys, P. Tailhades, Paramagnetic behaviour of silver nanoparticles generated by decomposition of silver oxalate, Solid State Sci. 69 (2017) 44–49, https://doi.org/10.1016/j.solidstatesciences.2017.05.009.

[7] Y. Yamamoto, T. Miura, Y. Nakae, T. Teranishi, M. Miyake, H. Hori, Magnetic properties of the noble metal nanoparticles protected by polymer, Phys. B: Condens. Matter 329–333 (Part 2) (2003) 1183–1184, https://doi.org/10.1016/s0921-4526(02)02102-6.

[8] K. de O. Santos, W.C. Elias, A.M. Signori, F.C. Giacomelli, H. Yang, J.B. Domingos, Synthesis and catalytic properties of silver nanoparticle–linear polyethylene imine colloidal systems, J. Phys. Chem. C 116 (7) (2012) 4594–4604, https://doi.org/10.1021/jp2087169.

[9] Y.S. Jeong, J.-B. Park, H.-G. Jung, J. Kim, X. Luo, J. Lu, L. Curtiss, K. Amine, Y.-K. Sun, B. Scrosati, Y.J. Lee, Study on the Catalytic Activity of Noble Metal Nanoparticles on Reduced Graphene Oxide for Oxygen Evolution Reactions in Lithium-Air Batteries, Nano Lett. 15 (7) (2015) 4261–4268, https://doi.org/10.1021/nl504425h.

[10] B. Zhao, I. Aravind, S. Yang, Z. Cai, Y. Wang, R. Li, S. Subramanian, P. Ford, D. R. Singleton, M.A. Gundersen, S.B. Cronin, Nanoparticle-Enhanced Plasma Discharge Using Nanosecond High-Voltage Pulses, J. Phys. Chem. C (2020), https://doi.org/10.1021/acs.jpcc.9b12054.

[11] K.H. Cho, J.E. Park, T. Osaka, S.G. Park, The study of antimicrobial activity and preservative effects of nanosilver ingredient, Electrochim. Acta 51 (2005) 956–960, https://doi.org/10.1016/j.electacta.2005.04.071.

[12] A.R. Shahverdi, A. Fakhimi, H.R. Shahverdi, S. Minaian, Synthesis and effect of silver nanoparticles on the antibacterial activity of different antibiotics against Staphylococcus aureus and Escherichia coli, Nanomed. Nanotechnol. Biol. Med. 3 (2007) 168–171, https://doi.org/10.1016/j.nano.2007.02.001.

[13] S. Kokura, O. Handa, T. Takagi, T. Ishikawa, Y. Naito, T. Yoshikawa, Silver nanoparticles as a safe preservative for use in cosmetics, Nanomed. Nanotechnol. Biol. Med. 6 (4) (2010) 570–574, https://doi.org/10.1016/j.nano.2009.12.002.

[14] J. Natsuki, T. Natsuki, Y. Hashimoto, A Review of Silver Nanoparticles: Synthesis Methods, Properties and Applications, Int. J. Mater. Sci. Appl. 4 (5) (2015) 325–332, https://doi.org/10.11648/j.ijmsa.20150405.17.

[15] J.L. Elechiguerra, J. Burt, J.R. Morones, A. Camacho-Bragado, X. Gao, H.H. Lara, M.J. Yacaman, Interaction of silver nanoparticles with HIV-1, J. Nanobiotechnol. 3 (2005) 6, https://doi.org/10.1186/1477-3155-3-6.

[16] J.M. Ashraf, M.A. Ansari, H.M. Khan, M.A. Alzohairy, I. Choi, Green synthesis of silver nanoparticles and characterization of their inhibitory effects on AGEs formation using biophysical techniques, Sci. Rep. 6 (1) (2016) 20414, https://doi.org/10.1038/srep20414.

[17] X.-F. Zhang, Z.-G. Liu, W. Shen, S. Gurunathan, Silver Nanoparticles: Synthesis, Characterization, Properties, Applications, and Therapeutic Approaches, Int. J. Mol. Sci. 17 (9) (2016) E1534, https://doi.org/10.3390/ijms17091534.

[18] S.R. Emory, S. Nie, Near-Field Surface-Enhanced Raman Spectroscopy on Single Silver Nanoparticles, Anal. Chem. 69 (14) (1997) 2631–2635, https://doi.org/10.1021/ac9701647.

[19] S.R. Emory, W.E. Haskins, S. Nie, Direct Observation of Size-Dependent Optical Enhancement in Single Metal Nanoparticles, J. Am. Chem. Soc. 120 (31) (1998) 8009–8010, https://doi.org/10.1021/ja9815677.
[20] N. Tyagi, S.K. Srivastava, S. Arora, Y. Omar, Z.M. Ijaz, A. AL-Ghadhban, S. K. Deshmukh, J.E. Carter, A.P. Singh, S. Singh, Comparative analysis of the relative potential of silver, zinc- oxide and titanium-dioxide nanoparticles against UVB-induced DNA damage for the prevention of skin carcinogenesis, Cancer Lett. 383 (1) (2016) 53–61, https://doi.org/10.1016/j.canlet.2016.09.026.
[21] S. Gajbhiye, S. Sakharwade, Silver Nanoparticles in Cosmetics, J. Cosmet. Dermatol. Sci. Appl. 6 (01) (2016) 48–53, https://doi.org/10.4236/jcdsa.2016.61007.
[22] F. Zhang, X. Wu, Y. Chen, H. Lin, Application of silver nanoparticles to cotton fabric as an antibacterial textile finish, Fibers Polym. 10 (4) (2009) 496–501, https://doi.org/10.1007/s12221-009- 0496-8.
[23] H. Wigger, Case study: Clothing textiles with incorporated silver nanoparticles, Environmental Release of and Exposure to Iron Oxide and Silver Nanoparticles, Springer Vieweg, Wiesbaden, 2017 doi: 10.1007/978-3-658-16791-2.
[24] K. Gudikandula, S.C. Maringanti, Synthesis of silver nanoparticles by chemical and biological methods and their antimicrobial properties, J. Exp. Nanosci. 11 (9) (2016) 714–721, https://doi.org/10.1080/17458080.2016.1139196.
[25] M. Zaarour, M. El Roz, B. Dong, R. Retoux, R. Aad, J. Cardin, C. Dufour, F. Gourbilleau, J.-P. Gilson, S. Mintova, Photochemical Preparation of Silver Nanoparticles Supported on Zeolite Crystals, Langmuir 30 (21) (2014) 6250–6256, https://doi.org/10.1021/la5006743.
[26] X. Zhang, E.M. Hicks, J. Zhao, G.C. Schatz, R.P. Van Duyne, Electrochemical Tuning of Silver Nanoparticles Fabricated by Nanosphere Lithography, Nano Lett. 5 (7) (2005) 1503–1507, https://doi.org/10.1021/nl050873x.
[27] J. Zhu, S. Liu, O. Palchik, Y. Koltypin, A. Gedanken, Shape-Controlled Synthesis of Silver Nanoparticles by Pulse Sonoelectrochemical Methods, Langmuir 16 (16) (2000) 6396–6399, https://doi.org/10.1021/la991507u.
[28] S. Iravani, H. Korbekandi, S.V. Mirmohammadi, B. Zolfaghari, Synthesis of silver nanoparticles: chemical, physical and biological methods, Res. Pharm. Sci 9 (6) (2014) 385–406.
[29] J. Siegel, O. Kvítek, P. Ulbrich, Z. Kolská, P. Slepička, V. Švorčík, Progressive approach for metal nanoparticle synthesis, Mater. Lett. 89 (2012) 47–50, https://doi.org/10.1016/j.matlet.2012.08.048.
[30] G.W. Yang, Laser ablation in liquids: Applications in the synthesis of nanocrystals, Prog. Mater. Sci. 52 (2007) 648–698, https://doi.org/10.1016/j.pmatsci.2006.10.016.
[31] C.-H. Tsai, P.-Y. Wang, I.-C. Lin, H. Huang, G.-S. Liu, C.-L. Tseng, Ocular Drug Delivery: Role of Degradable Polymeric Nanocarriers for Ophthalmic Application, Int. J. Mol. Sci. 19 (9) (2018) 2830, https://doi.org/10.3390/ijms19092830.
[32] V.K. Yellepeddi, S. Palakurthi, Recent advances in topical ocular drug delivery, J. Ocul. Pharmacol. Ther. 32 (2) (2016) 67–82, https://doi.org/10.1089/jop.2015.0047.
[33] R. Bisht, A. Mandal, J.K. Jaiswal, I.D. Rupenthal, Nanocarrier mediated retinal drug delivery: Overcoming ocular barriers to treat posterior eye diseases, Wiley Interdiscipl. Rev. Nanomed. Nanobiotechnol. 10 (2) (2018), e1473, https://doi.org/10.1002/wnan.1473.
[34] A. Rajapakshal, M. Fink, B.A. Todd, Size-dependent diffusion of dextrans in excised porcine corneal stroma, Mol. Cell Biomech. 12 (3) (2015) 215–230, https://doi.org/10.3970/mcb.2015.012.215.
[35] A.S. Nikolov, R.G. Nikov, I.G. Dimitrov, N.N. Nedyalkov, P.A. Atanasov, M. T. Alexandrov, D.B. Karashanova, Modification of the silver nanoparticles size-distribution by means of laser light irradiation of their water suspensions, Appl. Surf. Sci. 280 (2013) 55–59, https://doi.org/10.1016/j.apsusc.2013.04.079.
[36] H.M. Momen, Effects of particle size and laser wavelength on heating of silver nanoparticles under laser irradiation in liquid, Pramana, J. Phys. 87 (2016) 26, https://doi.org/10.1007/s12043-016-1233- 7.
[37] S. Inasawa, M. Sugiyama, Y. Yamaguchi, Laser-Induced Shape Transformation of Gold Nanoparticles below the Melting Point: The Effect of Surface Melting, J. Phys. Chem. B 109 (8) (2005) 3104–3111, https://doi.org/10.1021/jp045167j.
[38] M. Honda, Y. Saito, N.I. Smith, K. Fujita, S. Kawata, Nanoscale heating of laser irradiated single gold nanoparticles in liquid, Opt. Express 19 (13) (2011) 12375–12383, https://doi.org/10.1364/oe.19.012375.
[39] F. Mafuné, J.-Y. Kohno, Y. Takeda, T. Kondow, Dissociation and Aggregation of Gold Nanoparticles under Laser Irradiation, J. Phys. Chem. B 105 (38) (2001) 9050–9056, https://doi.org/10.1021/jp0111620.
[40] S. Link, M. El-Sayed, Spectral Properties and Relaxation Dynamics of Surface Plasmon Electronic Oscillations in Gold and Silver Nanodots and Nanorods, J. Phys. Chem. B 103 (40) (1999) 8410–8426, https://doi.org/10.1021/jp9917648.
[41] S. Link, M.A. El-Sayed, Shape and size dependence of radiative, non-radiative and photothermal properties of gold nanocrystals, Int. Rev. Phys. Chem. 19 (3) (2000) 409–453, https://doi.org/10.1080/01442350050034180.
[42] D. Catone, A. Ciavardini, L. Di Mario, A. Paladini, F. Toschi, A. Cartoni, I. Fratoddi, I. Venditti, A. Alabastri, R.P. Zaccaria, P. O'Keeffe, Plasmon Controlled Shaping of Metal Nanoparticle Aggregates by Femtosecond Laser-Induced Melting, J. Phys. Chem. Lett. 9 (17) (2018) 5002–5008, https://doi.org/10.1021/acs.jpclett.8b02117.
[43] V. Amendola, M. Meneghetti, Laser ablation synthesis in solution and size manipulation of noble metal nanoparticles, Phys. Chem. Chem. Phys. 11 (20) (2009) 3805–3821, https://doi.org/10.1039/b900654k.
[44] F. Giammanco, E. Giorgetti, P. Marsili, A. Giusti, Experimental and Theoretical Analysis of Photofragmentation of Au Nanoparticles by Picosecond Laser Radiation, J. Phys. Chem. C 114 (8) (2010) 3354–3363, https://doi.org/10.1021/jp908964t.
[45] A.M. Prokhorov, V.I. Konov, I. Ursu, I.N. Mihailescu, Laser Heating of Metals, Adam Hilger Ltd - The Publishing House of the Institute of Physics, (Bristol, England, UK, 1990), 1990, pp. 275.
[46] R.G. Nikov, A.S. Nikolov, P.A. Atanasov, Preparation of gold and silver nanoparticles by pulsed laser ablation of solid target in water, 16th International School on Quantum Electronics: Laser Physics and Application, Proc. SPIE 7747 (2011), https://doi.org/10.1117/12.881908.
[47] B. Balamurugan, T. Maruyama, Size-modified d bands and associated interband absorption of Ag nanoparticles, J. Appl. Phys. 102 (2007), 034306, https://doi.org/10.1063/1.2767837.
[48] A.S. Nikolov, N.E. Stankova, D.B. Karashanova, N.N. Nedyalkov, E.L. Pavlov, L.A. Avramov, K. Koev, Patent Application, Incoming number № 112999/24.09.2019 in Patent Office of Republic of Bulgaria, "Method for production of ultra-fine monodisperse nanoparticles with laser pulses", 2019.
[49] V. Amendola, O.M. Bakr, F. Stellacci, A Study of the Surface Plasmon Resonance of Silver Nanoparticles by the Discrete Dipole Approximation Method: Effect of Shape, Size, Structure, and Assembly, Plasmonics 5 (2010) 85–97, https://doi.org/10.1007/s11468-009-9120-4.
[50] U. Kreibig, M. Vollmer, Optical Properties of Metal Clusters, Springer, Heidelberg, 1995.
[51] A. Takami, H. Kurita, S. Koda, Laser-Induced Size Reduction of Noble Metal Particles, J. Phys. Chem. B 103 (8) (1999) 1226–1232, https://doi.org/10.1021/jp983503o.
[52] V. Amendola, M. Meneghetti, Size Evaluation of Gold Nanoparticles by UV−vis Spectroscopy, J. Phys. Chem. C 113 (11) (2009) 4277–4285, https://doi.org/10.1021/jp8082425.
[53] R.G. Nikov, A.S. Nikolov, N.N. Nedyalkov, I.G. Dimitrov, P.A. Atanasov, M. T. Alexandrov, Stability of contamination-free gold and silver nanoparticles produced by nanosecond laser ablation of solid targets in water, Appl. Surf. Sci. 258 (2012) 9318–9322, https://doi.org/10.1016/j.apsusc.2011.12.040.
[54] S. Chernousova, M. Epple, Silver as antibacterial agent: ion, nanoparticle, and metal, Angew. Chem. Int. Ed. Engl. 52 (6) (2013) 1636–1653, https://doi.org/10.1002/anie.201205923.
[55] L. Duta, C. Ristoscu, G.E. Stan, M.A. Husanu, C. Besleaga, M.C. Chifiriuc, V. Lazar, C. Bleotu, F. Miculescu, N. Mihailescu, E. Axente, M. Badiceanu, D. Bociaga, I. N. Mihailescu, New bio-active, animicrobial and adherent coatings of nanostructured carbon double-reinforced with silver and silicon by Matrix-Assisted Pulsed Laser Evaporation for medical applications, Appl. Surf. Sci. 441 (2018) 871–883, https://doi.org/10.1016/j.apsusc.2018.02.047.
[56] G. Socol, M. Socol, L. Sima, S. Petrescu, M. Enculescu, F. Sima, M. Miroiu, G. Popescu- Pelin, N. Stefan, R. Cristescu, C.N. Mihailescu, A. Stanculescu, C. Sutan, I.N. Mihailescu, Combinatorial pulsed laser deposition of Ag-containing calcium phosphate coatings, Digest J. Nanomater. Biostruct. 7 (2) (2012) 563–576.
[57] N. Hachicho, P. Hoffmann, K. Ahlert, H.J. Heipieper, Effect of silver nanoparticles and silver ions on growth and adaptive response mechanisms of Pseudomonas putida mt-2, FEMS Microbiol. Lett. 355 (1) (2014) 71–77, https://doi.org/10.1111/1574-6968.12460.